Muonic three-body Coulomb systems in the hyperspherical approach

M. Decker and W. Sandhas
Physikalisches Institut, Universität Bonn, D-53115 Bonn, Germany

V. B. Belyaev
Bogoliubov Laboratory of Theoretical Physics, Joint Institute for Nuclear Research, 141980 Dubna, Russia
(Received 30 June 1995)

Muonic three-body bound states and resonances are treated within a hyperspherical adiabatic expansion scheme. A new method for determining the basis functions of this expansion is developed: decomposing these functions into Faddeev-type components, an equivalent treatment of all two-body contributions, and thus the correct asymptotics, are guaranteed. This approach is characterized by its high symmetry and a considerable reduction of the numerical effort. Using partial wave and B-spline expansions for the components, wave functions and energies of the $dt\mu$ and $d^3\mathrm{He}\mu$ molecules are calculated in extreme and uncoupled adiabatic approximation. For $dt\mu$ good agreement with alternative calculations, which are based on a much higher number of expansion functions, is found, and the results for the $d^3\mathrm{He}\mu$ system are rather close to variational calculations.

PACS number(s): 36.10.Dr

I. INTRODUCTION

The investigation of muonic molecules, consisting of two nuclei and one negatively charged muon, is mainly motivated by the idea of muon catalyzed fusion (μCF). A lot of experiments and calculations have been done in order to determine the properties of such systems. Especially the bound states of the $dt\mu$ molecule, the most promising system for μCF, are known with high precision. Variational methods [1–4], hyperspherical approaches [5,6], and solutions of the Faddeev equations [7] were employed in this context.

In muonic three-body systems with nuclei of higher charge, as, e.g., $d^3\mathrm{He}\mu$, the possibility of μCF is considerably reduced due to the stronger Coulomb repulsion. But these states are of interest with respect to μCF kinetics [8], and hence some Born-Oppenheimer [9,10] and variational [11] calculations have been performed also for them. There is, however, a completely different reason for investigating such systems in more detail. In nuclear astrophysics, reactions of the type $d+{}^3\mathrm{He}\rightarrow{}^4\mathrm{He}+p$, $t+{}^4\mathrm{He}\rightarrow{}^7\mathrm{Li}+\gamma$ $p+{}^7\mathrm{Be}\rightarrow{}^8\mathrm{B}+\gamma$ play an important role, the first two in the primordial nucleosynthesis, the third one with respect to the solar neutrino problem. The Coulomb barrier prevents measuring the corresponding cross sections at astrophysical energies in direct collision experiments. One, therefore, had to rely up to now on low-energy extrapolations of existing data. However, when screening the positive charges by a negatively charged muon, these cross sections should become experimentally accessible. In other words, they should become measurable in processes of the type

$$d\mu+{}^3\mathrm{He}\rightarrow(d^3\mathrm{He}\mu)^*\rightarrow{}^4\mathrm{He}\mu+p,$$

$$t\mu+{}^4\mathrm{He}\rightarrow(t^4\mathrm{He}\mu)^*\rightarrow{}^7\mathrm{Li}\mu+\gamma$$

and

$$p\mu+{}^7\mathrm{Be}\rightarrow(p^7\mathrm{Be}\mu)^*\rightarrow{}^8\mathrm{B}\mu+\gamma.$$

As a first step towards the full treatment of such processes, we develop in the present paper a reliable method for calculating the muonic three-body bound states and resonances involved. This method is based on the standard expansion of the three-body wave function into surface functions [12,13]. The essential problem, thus, consists in constructing these functions, which is done in our approach by decomposing them into Faddeev-type components. Proceeding in this way, overcompleteness problems are avoided, all two-body subsystems are treated in an equivalent way, and the correct asymptotics is guaranteed. For the determination of the partial wave projected Faddeev-type components, B-spline expansions and the Galerkin technique [14] are employed.

In the present paper we develop our method and, in order to test its efficiency, apply it to the well-understood $dt\mu$ molecule and, as an example of systems of higher charge, to the $d^3\mathrm{He}\mu$ molecule. It turns out that, in comparison with an alternative hyperspherical treatment of $dt\mu$, [5], the number of expansion functions is considerably reduced. The energy obtained for the $d^3\mathrm{He}\mu$ resonance is somewhat different from the Born-Oppenheimer results [9,10] mentioned above, but agrees quite well with variational calculations [11], which are generally considered to be most accurate. These rather promising findings justify the application of our approach to more delicate problems as, e.g., the treatment of high-lying resonances in the $p^6\mathrm{Li}\mu$ or $p^7\mathrm{Be}\mu$ systems. The corresponding investigations will be presented in a subsequent publication.

The paper is organized as follows. In Sec. II we give a brief review of the hyperspherical adiabatic approximation. Section III contains a detailed description of our new approach to determining the surface functions. Section IV is devoted to the numerical treatment of the problem and presents the results obtained. The conclusions are drawn in Sec. V.

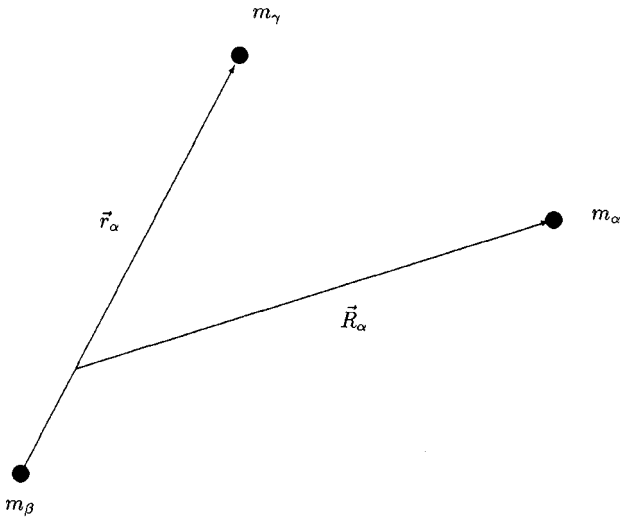

FIG. 1. Set α of Jacobi coordinates.

II. THE HYPERSPHERICAL ADIABATIC APPROACH

The motion of three particles in their center of mass system can be described in Jacobi coordinates $(\vec{r}_\alpha,\vec{R}_\alpha)$ as shown in Fig. 1. The index α specifies one of the three possible sets of coordinates, $\alpha=1$, 2, or 3. Particles 1 and 2 are the two nuclei, with particle 2 being the heavier one, and particle 3 is a negatively charged muon. The Hamiltonian of these particles, interacting only via the Coulomb force, is given by

$$H=-\frac{\hbar^2}{2}\left(\frac{1}{m_\beta}+\frac{1}{m_\gamma}\right)\Delta_{\vec{r}_\alpha}-\frac{\hbar^2}{2}\left(\frac{1}{m_\alpha}+\frac{1}{m_\beta+m_\gamma}\right)\Delta_{\vec{R}_\alpha}+\sum_{\alpha=1}^{3}\frac{Z_\beta Z_\gamma e^2}{|\vec{r}_\alpha|},\tag{1}$$

where m_α and Z_α denote the masses and charges of the particles, respectively, and (α,β,γ) is a cyclic permutation of (1,2,3). Appropriate units, when treating the Coulomb problem, are the Bohr radius a of one of the two-body subsystems and its ground-state energy ε. We take the system of particles 2 and 3, i.e., the heavier nucleus and the muon. Its Bohr radius $a^{(23)}$ and ground-state energy $\varepsilon^{(23)}$ are

$$a^{(23)}=\frac{\hbar^2(m_2+m_3)}{|Z_2Z_3|m_2m_3e^2},\quad \varepsilon^{(23)}=-\frac{\hbar^2(m_2+m_3)}{2m_2m_3[a^{(23)}]^2}.\tag{2}$$

Introducing dimensionless coordinates

$$\vec{x}_\alpha=\frac{c_\alpha}{a^{(23)}}\vec{r}_\alpha,\quad \vec{y}_\alpha=\frac{c_\alpha}{d_\alpha a^{(23)}}\vec{R}_\alpha,\tag{3}$$

where

$$c_\alpha=\sqrt{\frac{m_1(m_2+m_3)}{m_\alpha(m_\beta+m_\gamma)}},\quad d_\alpha=\sqrt{\frac{m_\beta m_\gamma(m_\alpha+m_\beta+m_\gamma)}{m_\alpha(m_\beta+m_\gamma)^2}},\tag{4}$$

the Hamiltonian reads, in units of $|\varepsilon^{(23)}|$,

$$H=-\Delta_{\vec{x}_\alpha}-\Delta_{\vec{y}_\alpha}-2Z_1\sum_{\beta=1}^{3}\frac{c_\beta}{Z_\beta|\vec{x}_\beta|}.\tag{5}$$

Instead of the variables $\vec{x}_\alpha$ and $\vec{y}_\alpha$, we use in what follows the hyperspherical coordinates $(\rho,\omega_\alpha,\hat{x}_\alpha,\hat{y}_\alpha)$ defined by

$$|\vec{x}_\alpha|=\rho\,\cos\omega_\alpha,\quad |\vec{y}_\alpha|=\rho\,\sin\omega_\alpha,\quad \hat{x}_\alpha=\frac{\vec{x}_\alpha}{|\vec{x}_\alpha|},\quad \hat{y}_\alpha=\frac{\vec{y}_\alpha}{|\vec{y}_\alpha|},\tag{6}$$

where $0\leqslant\rho<\infty$ and $0\leqslant\omega_\alpha\leqslant\pi/2$. The hyperradius $\rho=\sqrt{\vec{x}_\alpha^2+\vec{y}_\alpha^2}$ is a measure for the size of the three-body system, the hyperangle ω_α is determined by the ratio between $|\vec{y}_\alpha|$ and $|\vec{x}_\alpha|$. Due to the choice of the factors in (3), the hyperradius does not depend on the set of Jacobi coordinates. Only the five angles $\Omega_\alpha=(\omega_\alpha,\hat{x}_\alpha,\hat{y}_\alpha)$ depend on the specific set of coordinates α. Since the five angles of one set can be transformed into the angles of another one by a kinematic rotation, we omit the corresponding indices, if they are not necessary for the argumentation. In the coordinates (6), the Hamiltonian takes the well-known form

$$H=-\rho^{-5/2}\frac{\partial^2}{\partial\rho^2}\rho^{5/2}+\frac{\Lambda^2(\Omega)}{\rho^2}+\frac{\mathscr{V}(\Omega)}{\rho}.\tag{7}$$

Here the grand angular momentum operator Λ is given by

$$\Lambda^2(\Omega_\alpha)=-\frac{1}{\cos\omega_\alpha\,\sin\omega_\alpha}\frac{\partial^2}{\partial\omega_\alpha^2}\cos\omega_\alpha\,\sin\omega_\alpha+\frac{\vec{l}_{\hat{x}_\alpha}^2}{\cos^2\omega_\alpha}+\frac{\vec{l}_{\hat{y}_\alpha}^2}{\sin^2\omega_\alpha}-\frac{1}{4},\tag{8}$$

where $\vec{l}_{\hat{x}_\alpha}$ and $\vec{l}_{\hat{y}_\alpha}$ are the subsystem angular momentum operators,

$$\vec{l}_{\hat{x}_\alpha}=\vec{x}_\alpha\times\frac{1}{i}\vec{\nabla}_{x_\alpha},\quad \vec{l}_{\hat{y}_\alpha}=\vec{y}_\alpha\times\frac{1}{i}\vec{\nabla}_{y_\alpha}.\tag{9}$$

The angular part of the three-body Coulomb potential reads

$$\mathscr{V}(\Omega)=\sum_{\alpha=1}^{3}\mathscr{V}_\alpha(\omega_\alpha)=-2Z_1\sum_{\alpha=1}^{3}\frac{c_\alpha}{Z_\alpha\cos\omega_\alpha}.\tag{10}$$

According to Macek [12], the six-dimensional Schrödinger equation,

$$H\Psi(\rho,\Omega)=E\Psi(\rho,\Omega),\tag{11}$$

is treated by solving first the corresponding five-dimensional angular problem and then the resulting one-dimensional radial equation. That is, we consider first the Hamiltonian (7) for fixed values of the hyperradius,

$$H_\rho(\Omega)=\frac{\Lambda^2(\Omega)}{\rho^2}+\frac{\mathscr{V}(\Omega)}{\rho}.\tag{12}$$

The corresponding eigenvalue equation,

$$H_\rho(\Omega)B_n(\rho,\Omega)=U_n(\rho)B_n(\rho,\Omega),\tag{13}$$

is a differential equation with respect to the five angular variables, while the hyperradius ρ enters merely as a parameter. Therefore, the eigenvalues $U_n(\rho)$, conventionally referred to as *eigenpotentials* [15], are ρ dependent. The operator $H_\rho(\Omega)$ has been shown to be self-adjoint with a purely discrete spectrum [16]. Its eigenfunctions $B_n(\rho,\Omega)$, denoted as *surface functions* [13], hence form a complete orthogonal set on the hypersphere, their normalization being chosen as

$$\langle B_m(\rho)|B_n(\rho)\rangle=\int d\Omega B_m^*(\rho,\Omega)B_n(\rho,\Omega)=\delta_{mn}. \tag{14}$$

Expanding now the three-body wave function $\Psi(\rho,\Omega)$ in terms of $B_n(\rho,\Omega)$,

$$\Psi(\rho,\Omega)=\sum_{n=1}^{\infty}\frac{f_n(\rho)}{\rho^{5/2}}B_n(\rho,\Omega), \tag{15}$$

the Schrödinger equation (11) goes over to

$$f_n''(\rho)=[U_n(\rho)-E]f_n(\rho)-\sum_{m=1}^{\infty}[2\langle B_n(\rho)|B_m'(\rho)\rangle f_m'(\rho)+\langle B_n(\rho)|B_m''(\rho)\rangle f_m(\rho)]. \tag{16}$$

Here, the coupling matrix elements are given by

$$\langle B_n(\rho)|B_m'(\rho)\rangle=\int d\Omega B_n^*(\rho,\Omega)\frac{\partial}{\partial\rho}B_m(\rho,\Omega) \tag{17}$$

and

$$\langle B_n(\rho)|B_m''(\rho)\rangle=\int d\Omega B_n^*(\rho,\Omega)\frac{\partial^2}{\partial\rho^2}B_m(\rho,\Omega). \tag{18}$$

Taking into account Eq. (14), the normalization condition $\langle\Psi|\Psi\rangle=1$ for the bound-state solutions of Eq. (11) reduces to

$$\sum_{n=1}^{\infty}\int_0^{\infty}d\rho|f_n(\rho)|^2=1. \tag{19}$$

The truncation of Eqs. (15), (16), and (19) to a finite number of terms $N>1$ or to a single term $N=1$ is called *coupled adiabatic approximation* (CAA) or *uncoupled adiabatic approximation* (UAA), respectively. In the latter case Eq. (16) simplifies to

$$f_n''(\rho)=[U_n(\rho)+\langle B_n'(\rho)|B_n'(\rho)\rangle-E]f_n(\rho). \tag{20}$$

Neglecting additionally the derivatives of the surface functions with respect to the hyperradius, we end up with the *extreme adiabatic approximation* (EAA),

$$f_n''(\rho)=[U_n(\rho)-E]f_n(\rho). \tag{21}$$

For the ground-state energies obtained in these approximations the following inequalities hold [17]

$$E^{\mathrm{EAA}}\leqslant E^{\mathrm{exact}}\leqslant E^{\mathrm{CAA}}\leqslant E^{\mathrm{UAA}}. \tag{22}$$

In the present paper, we restrict ourselves to the UAA and EAA, so that upper and lower bounds for the exact energy are found.

III. DETERMINATION OF THE SURFACE FUNCTIONS

Our main task consists in solving the five-dimensional eigenvalue equation (13). For this purpose an efficient expansion of its solutions, i.e., of the surface functions $B_n(\rho,\Omega)$, will be developed. Most essential is that this expansion satisfies the correct asymptotic properties.

At *small* hyperradii the grand angular momentum term with its ρ^{-2} behavior represents the dominant part in the operator (12). Hence, Eq. (13) reduces to

$$[\Lambda^2(\Omega)-\rho^2U_n(\rho)]B_n(\rho,\Omega)\rightsquigarrow 0 \quad \text{for } \rho\to 0. \tag{23}$$

By comparing this relation with the eigenvalue equation of the grand angular momentum operator,

$$[\Lambda^2(\Omega)-\mathscr{L}(\mathscr{L}+1)]Y_{[\mathscr{L}]}(\Omega)=0, \tag{24}$$

we obtain

$$U_n(\rho)\rightsquigarrow\frac{\mathscr{L}(\mathscr{L}+1)}{\rho^2},\quad B_n(\rho,\Omega)\rightsquigarrow Y_{[\mathscr{L}]}(\Omega)\quad\text{for }\rho\to 0. \tag{25}$$

Here, the $Y_{[\mathscr{L}]}(\Omega)$ are the hyperspherical harmonics [18] given by

$$Y_{[\mathscr{L}]}(\Omega_\alpha)=N_{[\mathscr{L}]}\cos^{l_\alpha}\omega_\alpha\sin^{L_\alpha}\omega_\alpha P_k^{(L_\alpha+1/2,l_\alpha+1/2)}\times(\cos 2\omega_\alpha)\mathscr{Y}_{l_\alpha L_\alpha}^{LM}(\hat{x}_\alpha,\hat{y}_\alpha), \tag{26}$$

where $N_{[\mathscr{L}]}$ is a normalization constant, $P_k^{(\alpha,\beta)}(x)$ a Jacobi polynomial, and $\mathscr{Y}_{l_\alpha L_\alpha}^{LM}(\hat{x}_\alpha,\hat{y}_\alpha)$ an eigenfunction of the squared total angular momentum operator $\vec{L}^2$, the so-called bispherical harmonic

$$\mathscr{Y}_{l_\alpha L_\alpha}^{LM}(\hat{x}_\alpha,\hat{y}_\alpha)=\sum_{m_\alpha M_\alpha}\langle l_\alpha m_\alpha L_\alpha M_\alpha|LM\rangle Y_{l_\alpha m_\alpha}(\hat{x}_\alpha)\times Y_{L_\alpha M_\alpha}(\hat{y}_\alpha), \tag{27}$$

with the Clebsch-Gordan coefficients $\langle l_\alpha m_\alpha L_\alpha M_\alpha|LM\rangle$ and the usual spherical harmonics $Y_{lm}(\hat{x})$. The index $[\mathscr{L}]$ of the hyperspherical harmonics collectively denotes the set of quantum numbers $\{k,l_\alpha,L_\alpha,L,M\}$. The eigenvalue in (24) is given by $\mathscr{L}=l_\alpha+L_\alpha+2k+\frac{3}{2}$. If it is degenerate we have in (25), instead of a single $Y_{[\mathscr{L}]}(\Omega)$, a linear combination of hyperspherical harmonics belonging to this value of $\mathscr{L}$.

At *large* hyperradii, and at energies below the three-body breakup threshold, the surface functions go over to *channel functions* [19], i.e., to products of muonic two-body bound states and free wave functions describing the motion of the respective third particle. The eigenpotentials converge towards the corresponding two-body binding energies $\varepsilon_m^{(\alpha 3)}$, $\alpha=1$ or 2 (note that particle 3 was assumed to be the muon). That is,

$$U_n(\rho)\to\varepsilon_m^{(\alpha 3)}\quad\text{for }\rho\to\infty \tag{28}$$

and

$$B_n(\rho,\Omega)\rightsquigarrow\rho^{3/2}\mathscr{R}_{ml_\beta}(\rho\,\cos\omega_\beta)\sin^{L_\beta}\omega_\beta\mathscr{Y}^{LM}_{l_\beta L_\beta}(\hat{x}_\beta,\hat{y}_\beta)$$

$$\text{for } \rho\to\infty, \quad (29)$$

where $\mathscr{R}_{ml_\beta}(\rho\,\cos\omega_\beta)$ represents the hydrogenlike wave function of the corresponding muonic atom with the principal quantum number m and the angular quantum number l_β,

$$\mathscr{R}_{ml_\beta}(\rho\,\cos\omega_\beta)=N_{ml_\beta}e^{-\sqrt{|\varepsilon_m^{(\alpha 3)}|}\rho\,\cos\omega_\beta}\times(2\sqrt{|\varepsilon_m^{(\alpha 3)}|}\rho\,\cos\omega_\beta)^{l_\beta}\times L_{m+l_\beta}^{2l_\beta+1}(2\sqrt{|\varepsilon_m^{(\alpha 3)}|}\rho\,\cos\omega_\beta). \quad (30)$$

$L_{m+l}^{2l+1}(x)$ is a Laguerre polynomial and N_{ml_β} a normalization constant. Consistently with Fig. 1, the channel index $\beta=1$ or 2 denotes the asymptotic (23,1) or (13,2) fragmentations, respectively. The $U_n(\rho)$ are labeled by $n=1,2,3,\ldots$ according to the increasing sequence of their asymptotic values $\varepsilon_m^{(\alpha 3)}$. Let us assume, e.g., that this sequence is $\varepsilon_1^{(23)}<\varepsilon_1^{(13)}<\varepsilon_2^{(23)}<\cdots$, as is the case for the $dt\mu$ system, then $U_1(\rho)\to\varepsilon_1^{(23)}$, $U_2(\rho)\to\varepsilon_1^{(13)}$, $U_3(\rho)\to\varepsilon_2^{(23)}$, . . . , and an analogous correspondence holds for $B_n(\rho,\Omega)$ and $\mathscr{R}_{ml_\beta}(\rho\,\cos\omega_\beta)$ in (29).

Considering (29) it becomes clear why expansions into hyperspherical harmonics, which are a good choice at small ρ, fail to reproduce the surface functions at large values of the hyperradius. Let us regard, for example, the ground state of the muonic atom ($m=1,l_1=0$). The atomic wave function $\mathscr{R}_{10}(\rho\,\cos\omega_1)$ has its maximal value at $\rho\,\cos\omega_1=a^{(23)}$, i.e., at the Bohr radius of this atom. For increasing ρ the corresponding ω_1 tends more and more towards $\pi/2$. That means, the wave function, regarded as a function of the hyperangle ω_1, shows a peak at $\omega_1\approx\pi/2$, which becomes sharper with increasing hyperradii. Such a peak structure, however, requires for its approximation a drastically increasing number of Jacobi polynomials, and thus of hyperspherical harmonics (26). Therefore, at large values of ρ an alternative expansion has to be chosen in correspondence with the asymptotic behavior (29). According to the above discussion, the channel functions, i.e., the right-hand side of (29), appear as an adequate basis set.

A natural way of reproducing both asymptotic regions seems to be to expand the surface functions both into hyperspherical harmonics and channel functions. The overcompleteness of such a basis, however, leads to serious problems when solving the corresponding generalized eigenvalue problem numerically. In fact, the channel functions, being orthogonal in the limit $\rho\to\infty$, become nonorthogonal, and in practice even linearly dependent, for decreasing ρ. As compared to the treatment of H^- in Ref. [19], this is more critical in our case, where we have to deal with two different muonic atoms, i.e., with two different sets of channel functions. When incorporating the strong interaction, such an expansion is needed also with respect to the third fragmentation (12,3). As a consequence, linear dependence occurs not only within one set but also between these two or three sets of functions, and the matrix associated with the metric of the expansion scheme becomes singular. To overcome this problem, only handmade constructions have been used up to now, which are based on introducing cutoff functions [5,20] or neglecting the small eigenvalues of the overlap matrix [21]. These methods, however, are not free of a certain arbitrariness in choosing the cutoff points or selecting the small eigenvalues, and therefore appear somewhat questionable.

A possible way out of these complications is suggested by the experiences of the three-nucleon problem. There, one encounters a rather similar situation: due to the identity of the particles, all sets of Jacobi coordinates are involved, which is most naturally taken care of by employing the Faddeev decomposition [22,23] of the three-body wave function. Adopting this idea, we split the surface functions into Faddeev-type components, combining thus the advantages of the adiabatic approximation and of the Faddeev approach. That is, we represent the surface functions as a superposition,

$$B_n(\rho,\Omega)=\sum_{\alpha=1}^{3} b_{\alpha n}(\rho,\Omega_\alpha), \quad (31)$$

of three components

$$b_{\alpha n}=G_0\zeta_\alpha V_\alpha B_n, \quad (32)$$

the Green function G_0 being defined by

$$G_0^{-1}=U_n-\frac{\Lambda^2}{\rho^2}+\sum_{\beta=1}^{3} V_\beta[\zeta_\beta-1]. \quad (33)$$

Note that by introducing the functions $\zeta_\alpha(\rho,\Omega_\alpha)$ we have taken over a modification of the original Faddeev definition as suggested in Refs. [24,25]. It is easily seen that with the definitions (32) and (33) the decomposition (31) satiesfies Eq. (13) for any choice of these functions. Following the proposal in [25] we choose in what follows

$$\zeta_\alpha(x_\alpha,y_\alpha)=2\left[1+\exp\left(\frac{(x_\alpha/x_0)^\nu}{y_\alpha/y_0+1}\right)\right]^{-1}, \quad (34)$$

with open parameters x_0, y_0, and ν. In the partial wave expansion applied in the following calculation, these parameters are used to accelerate the convergence. Inserting Eqs. (31)–(33) into (13) we end up with the following set of coupled equations:

$$\left[\frac{\Lambda^2}{\rho^2}+\frac{\mathscr{V}}{\rho}-\frac{1}{\rho}\sum_{\beta\neq\alpha}\zeta_\beta\mathscr{V}_\beta\right]b_{\alpha n}+\frac{\zeta_\alpha\mathscr{V}_\alpha}{\rho}\sum_{\beta\neq\alpha}b_{\beta n}=U_n b_{\alpha n}. \quad (35)$$

The remaining task now consists in determining the Faddeev-type components $b_{\alpha n}(\rho,\Omega_\alpha)$. Since we consider in the present paper only the Coulomb interaction between the three particles, the two nuclei involved cannot occur in a bound state. This suggests to use only two Faddeev-type components, b_{1n} and b_{2n}, reducing in this way the dimension of the coupled system of equations (35) correspondingly. When incorporating the strong interaction between the two nuclei, as is our goal in the long run, it appears natural to take into account also the third component b_{3n}.

Within the present formulation the restriction to two components is most easily achieved by putting $\zeta_3=0$. The set of equations (35) then simplifies to

$$\left[\frac{\Lambda^2}{\rho^2}+\frac{\mathscr{V}-\zeta_2\mathscr{V}_2}{\rho}\right]b_{1n}+\frac{\zeta_1\mathscr{V}_1}{\rho}b_{2n}=U_n b_{1n} \tag{36}$$

and

$$\left[\frac{\Lambda^2}{\rho^2}+\frac{\mathscr{V}-\zeta_1\mathscr{V}_1}{\rho}\right]b_{2n}+\frac{\zeta_2\mathscr{V}_2}{\rho}b_{1n}=U_n b_{2n}. \tag{37}$$

We emphasize once more that the general relations (35) are valid for any choice of ζ_α. Their specialization to Eqs. (36) and (37), therefore, is no approximation.

In the following calculations we use for the two components b_{1n} and b_{2n} the ansatz

$$\begin{aligned} b_{\alpha n}(\rho,\Omega_\alpha)=&e^{-\sqrt{|\epsilon_m|}\ \rho\ \cos\omega_\alpha} \\ &\times\sum_{l_\alpha L_\alpha i_\alpha} k_{\alpha l_\alpha L_\alpha i_\alpha n}(\rho)\cos^{l_\alpha}\omega_\alpha\ \sin^{L_\alpha}\omega_\alpha \\ &\times S_{i_\alpha}(\omega_\alpha)\mathscr{Y}^{LM}_{l_\alpha L_\alpha}(\hat{x}_\alpha,\hat{y}_\alpha)\quad . \end{aligned} \tag{38}$$

Here, the $\mathscr{Y}^{LM}_{l_\alpha L_\alpha}(\hat{x}_\alpha,\hat{y}_\alpha)$ are the eigenstates (27) of the squared total angular momentum operator. The dependence of the hyperangle is treated via an expansion into B-splines $S_{i_\alpha}(\omega_\alpha)$. The further functions of ω_α in (38) have been chosen in accord with the asymptotic properties discussed above: the Laguerre polynomial contained in (30) can be approximated by a sufficiently small number of splines, but this is not the case for the exponential function $e^{-\sqrt{|\epsilon_m|}\ \rho\ \cos\omega_\alpha}$, which therefore has been split off explicitly in (38). The additional factors $\sin^{L_\alpha}\omega_\alpha$ and $\cos^{l_\alpha}\omega_\alpha$ reproduce the correct behavior near the points $\omega_\alpha\approx 0$ and $\omega_\alpha\approx\pi/2$, respectively. Since the Jacobi polynomial in (26) can be expanded quite well into splines, ansatz (38) is also appropriate in the region of small values of the hyperradius.

Inserting the ansatz (38) into (36) and (37) and projecting onto the partial waves $\langle l_1L_1LM|$ and $\langle l_2L_2LM|$, respectively, we end up with the generalized eigenvalue problem

$$\begin{aligned} &\sum_{\beta l_\beta L_\beta i_\beta}\mathscr{A}^{\alpha l_\alpha L_\alpha}_{\beta l_\beta L_\beta i_\beta n}(\rho,\omega_\alpha)k_{\beta l_\beta L_\beta i_\beta n}(\rho) \\ &\quad=U_n(\rho)\sum_{\beta l_\beta L_\beta i_\beta}\mathscr{B}^{\alpha l_\alpha L_\alpha}_{\beta l_\beta L_\beta i_\beta n}(\rho,\omega_\alpha)k_{\beta l_\beta L_\beta i_\beta n}(\rho), \end{aligned} \tag{39}$$

providing us with the expansion coefficients $k_{\alpha l_\alpha L_\alpha i_\alpha n}(\rho)$ and the eigenvalues $U_n(\rho)$. Note that, as in the original relation (13), the hyperradius ρ occurs here as a parameter. Explicit formulas for the matrices $\mathscr{A}$ and $\mathscr{B}$ are given in the Appendix.

IV. NUMERICAL TREATMENT AND RESULTS

In the following numerical investigations we restrict ourselves to states of total angular momentum $L=0$, which implies identical values of the subsystem and the relative angular momenta l_α and L_α, respectively. Convergence has been achieved when choosing their maximal value as $l_{\max}=10$. It turns out that in ansatz (38) 20 B-splines $S_i(\omega_\alpha)$ are sufficient to obtain stable results. In order to reproduce the peak structure at $\omega_\alpha\approx\pi/2$, a fairly small mesh of spline nodes had to be chosen in this region.

To get rid of the hyperangle ω_α in Eq. (39), which its solutions $k_{\alpha l_\alpha L_\alpha i_\alpha n}(\rho)$ and $U_n(\rho)$ do not depend on, two different methods have been developed. In the so-called *collocation point method* [26] Eq. (39) is solved at specific values of the hyperangle. In order to obtain a quadratic eigenvalue problem, only a limited number of these collocation points is allowed. In the *Galerkin method* [14], analogously to partial wave projections, Eq. (39) is multiplied with the expansion functions $S_j(\omega_\alpha)$ and integrated over the hyperangle. The resulting eigenvalue problem remains quadratic for any number of integration points, which allows us to choose 20 mesh points for each spline, while the collocation method would

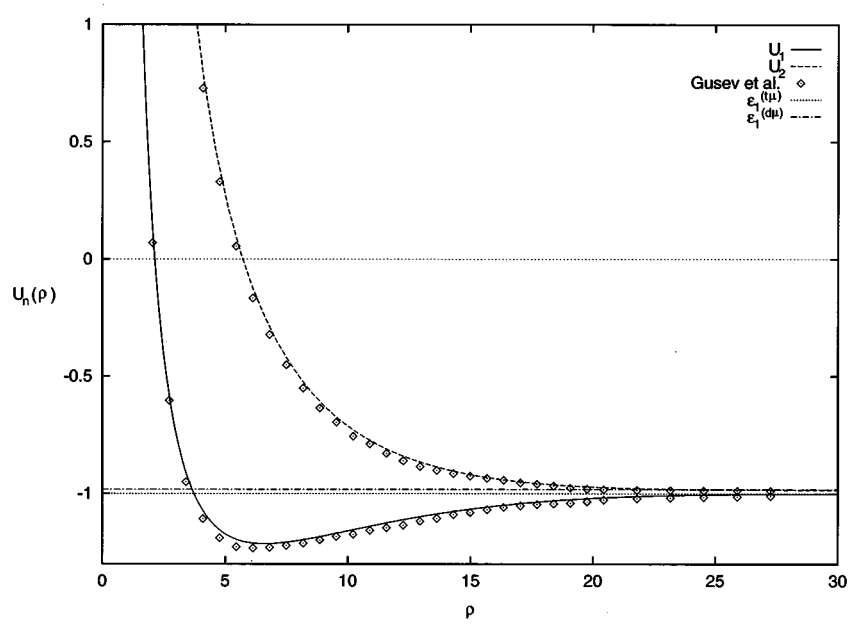

FIG. 2. Lowest eigenpotentials $U_1(\rho)$ and $U_2(\rho)$ of the $dt\mu$ system for $L=0$. With increasing hyperradius they converge towards the ground-state energies $\varepsilon_1^{(t\mu)}$ and $\varepsilon_1^{(d\mu)}$, respectively. The diamonds are the results of Ref. [5].

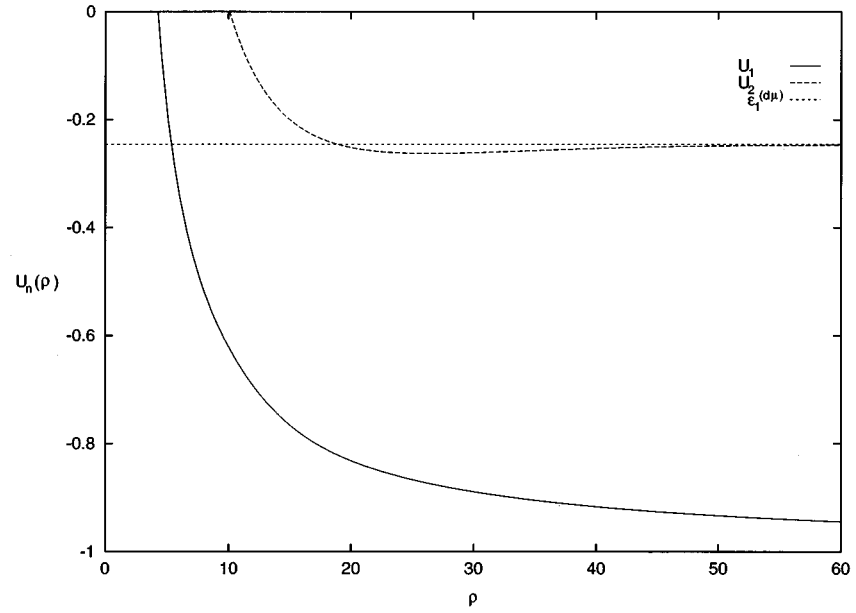

FIG. 3. Lowest eigenpotentials $U_1(\rho)$ and $U_2(\rho)$ of the $d^3\mathrm{He}\mu$ system for $L=0$. They converge towards the ground-state energies $\varepsilon_1^{(\mathrm{He}\,\mu)}=-1$ and $\varepsilon_1^{(d\mu)}$, respectively.

restrict us to two or three points only. The consequence is a higher stability of the Galerkin method, a feature particularly relevant for the treatment of the singularity of the Coulomb potential at the origin. Moreover, an appropriate transformation of the mesh points [27] is used in this context. The integrations over the hyperangle ω_α and the angle between $\vec{x}_\alpha$ and $\vec{y}_\alpha$ [see Eq. (46)] are performed via Gaussian quadrature.

Choosing 2 Faddeev-type components, 11 partial waves, and 20 B-splines, we end up with a (440×440)- dimensional eigenvalue problem. For its solutions the Lanczos algorithm is employed, using the trick of shifted equations described in [28]. This powerful tool replaces the original (440×440)-dimensional problem by an effective 7×7 matrix equation.

In Fig. 2 the two lowest eigenpotentials of the $dt\mu$ system are shown together with the results of Gusev *et al.* [5]. The latter ones have been read off simply from the corresponding figure in [5], with the size of the diamonds indicating the reading error. It is seen that with only 440 basis functions we practically reproduce the results of Gusev *et al.*, who needed more than 1800 functions. The decomposition of the surface functions into Faddeev-type components, thus, leads to a considerable reduction of the numerical effort.

Figure 3 shows the corresponding eigenpotentials of the $d^3\mathrm{He}\mu$ system. In contrast to the $dt\mu$ case, the lowest potential is purely repulsive, as expected in view of the Coulomb repulsion between the deuteron and the $^3\mathrm{He}\mu$ subsystem. The attractive character of the second eigenpotential is a consequence of the polarization of the $d\mu$ atom in the Coulomb field of the ^{3}He nucleus.

In Fig. 4 we make this statement explicit by presenting the relevant partial wave contributions to the second eigen-

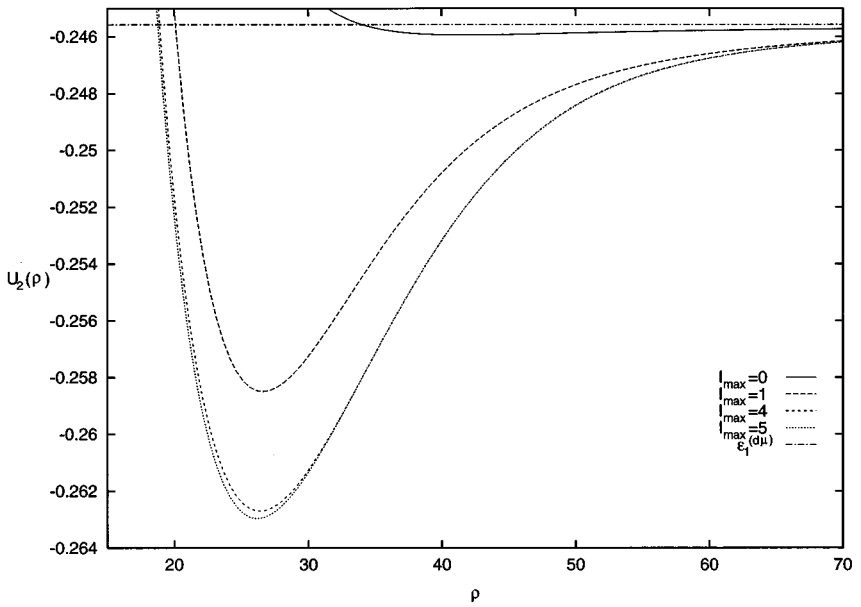

FIG. 4. Second eigenpotential of $d^3\mathrm{He}\mu$ for different values of $l_{\max}$, i.e., for different numbers of partial waves taken into account.

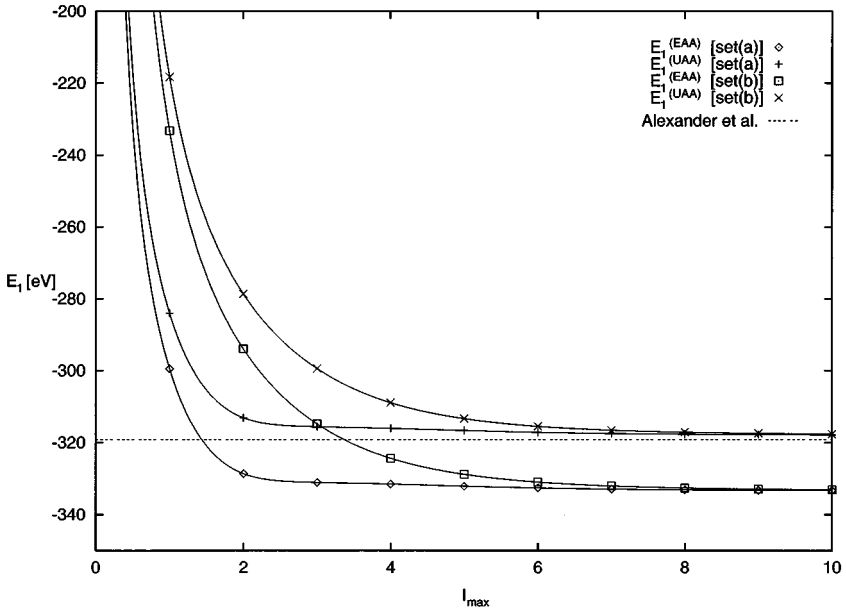

FIG. 5. Binding energies of the ground state of $dt\mu$ ($L=0$) obtained for different values of $l_{\max}$. The lines serve to guide the eye. The dashed line is the result of the variational calculation [1]. The two curves converging towards a value somewhat above this line correspond to the UAA. The two lower curves represent the EAA results. In both approximations the two sets of parameters of Table I are used.

potential. Choosing $l_{\max}=0$, thus enforcing the atom to be in an isotropic state, nearly no attraction is seen. This changes drastically when taking into account anisotropic contributions. The main part of the attraction is given already by the p-wave ($l_{\max}=1$), but attractive contributions are provided also by the higher partial waves up to $l_{\max}=4$ or 5.

The radial equations are treated both within the extreme and the uncoupled adiabatic approximations (21) and (20), making use of a Runge-Kutta algorithm. By inserting (25) into (21) and (20) one infers for some $\rho_0 \ll 1$ the boundary condition

$$\rho_0 f_n'(\rho_0)=(\mathscr{L}+1) f_n(\rho_0). \tag{40}$$

We choose $\rho_0=10^{-3}$ and integrate the radial equation up to 80 or 160 Bohr radii in case of the $dt\mu$ or $d^3\mathrm{He}\mu$ molecules, respectively. Since only the attractive eigenpotentials produce bound states or resonances, the radial equations have been solved with $U_1(\rho)$ for $dt\mu$ and $U_2(\rho)$ for $d^3\mathrm{He}\mu$.

In Fig. 5 we show the resulting ground-state binding energies for the $dt\mu$ molecule as a function of the number of subsystem partial waves taken into account. The two lower (upper) curves correspond to the EAA (UAA), yielding overbinding (underbinding) in comparison with the variational calculation [1]. These numerical results, hence, are in accord with the inequalities (22). The two curves belonging to the same approximation are calculated by using different sets of parameters ν, x_0, and y_0 (see Table I). As emphasized repeatedly, the exact solution of Eq. (13) is independent of the ζ_α and thus of these parameters. In practice this can be used as a means to test the quality of different approximations, in particular the convergence of the partial wave decompositions involved. The curves for the two different sets of parameters given in Table I agree for $l_{\max}=10$. But the corresponding final value is approached much faster with set(a). In this way the number of relevant partial waves can be reduced from $l_{\max}=10$ to about 7.

TABLE I. Two sets of parameters for the functions $\zeta_{1,2}$.

	ν	x_0	y_0
set(a)	2.3	1.3	10
set(b)	2.6	1.8	10

For the excited state of the $dt\mu$ molecule one encounters a rather similar situation, as demonstrated in Fig. 6. In this case the inequalities (22) have not yet been proved, but they are satisfied by the present numerical results: the EAA gives overbinding, while the binding obtained in UAA is somewhat too weak.

Table II presents a quantitative comparison between our results and the ones of Gusev *et al.* [5] and of a variational calculation [1]. The relative difference to the results of Ref. [1] is given in percent. It is seen that the extreme adiabatic approximation is justified only in the treatment of the ground state. The most important point in this table, however, is the very good agreement between our UAA results and the UAA results of Gusev *et al.* The remaining discrepancy to the variational calculations, thus, is not due to any inaccuracy in determining the surface functions, but arises from the uncoupled adiabatic approximation itself. Indeed, Gusev *et al.* showed that, going over to the coupled adiabatic approximation, it needs six surface functions to reproduce the variational calculations up to the first three significant digits. Our purpose, however, was not to redo this calculation, but to develop a better method for determining the surface functions, a method that should be well suited for the treatment of systems of higher mass and charge.

The binding energies obtained for the $d^3\mathrm{He}\mu$ system are given in Table III. We list there also the results of one-channel Born-Oppenheimer calculations [9,10] and of a variational calculation [11]. While the EAA gives a 10% stronger binding, the UAA differs less than 0.5% from the variational calculations. It also agrees better with these calculations than the Born-Oppenheimer results.

In the present one-channel adiabatic approximations (20) or (21), the radial equation yields for the $d^3\mathrm{He}\mu$ system a

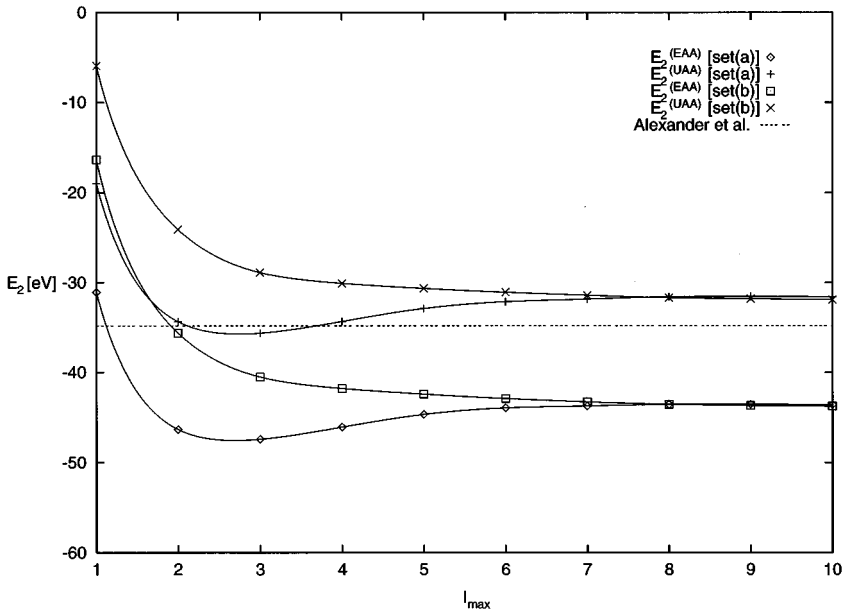

FIG. 6. Same as Fig. 5, but for the excited state of $dt\mu$.

bound state, which, however, can decay into the energetically lower channel $^3\mathrm{He}\mu + d$ when switching on the neglected coupling. Since the coupling is known to be weak [29,30], one expects this resonance to be fairly sharp and to appear almost at the binding energy found in the one-channel calculation.

V. CONCLUSIONS AND OUTLOOK

We have presented a method for calculating three-body Coulomb problems that combines the advantages of hyperspherical and Faddeev techniques.

The hyperspherical method allows one to separate the hyperradial motion from the angular part. After partial wave decomposition, this part consists of an equation in only one variable, the hyperangle, which was solved in the present investigations via an appropriate spline expansion. From the angular equation one gets, in particular, the eigenpotentials which play the role of effective potentials in the radial equation. The characteristic features of the respective problem, e.g., the occurrence of bound states and resonances as well as polarizability effects, can be inferred immediately from these potential curves. A further advantage is that, by solving the radial equation, upper and lower bounds are obtained for the binding energy of the ground state.

When combining the hyperspherical method with the Faddeev technique, we have made use of the typical property of Faddeev-type equations to treat all two-body contributions in an equivalent manner. Proceeding in this way allowed us to incorporate the two-body bound states explicitly without ending up with overcompleteness problems. Being physically motivated, this technique also led to a considerable reduction of the numerical effort.

The efficiency of our approach was demonstrated by studying the $dt\mu$ and $d^3\mathrm{He}\mu$ molecules or molecular resonances, but for systems of charge $Z>2$ complete convergence of the spline expansion has not yet been reached. Making use of Kato's cusp condition [31] it should be possible to overcome this problem. In Ref. [32] a considerable improvement of the convergence was, in fact, achieved. We expect that with this additional modification systems like $p^7\mathrm{Be}\mu$, which we are particularly interested in for reasons discussed in the Introduction, can be treated in a reliable manner.

Our procedure should allow us to treat also the scattering problem below the breakup threshold. In order to do this, only the boundary conditions for the radial equations have to be changed. Since the angular part does not depend on such boundary conditions, the rest of the formalism, especially the determination of the surface functions, remains unmodified.

ACKNOWLEDGMENTS

One of the authors (V.B.B.) would like to thank the Physikalisches Institut der Universität Bonn for its hospitality and two of them (V.B.B. and W.S.) acknowledge financial support by the Scientific Division of NATO, Research Grant No.

TABLE II. Binding energies of $dt\mu$ for $L=0$.

	Ground state		Excited state	
Method	E_1 (eV)	$\Delta E_1/E_1$ (%)	E_2 (eV)	$\Delta E_2/E_2$ (%)
EAA	−333.09	+4.37	−43.76	+25.6
UAA	−317.60	−0.48	−31.90	−8.43
UAA [5]	−317.78	−0.43	−32.14	−7.72
Variational [1]	−319.14		−34.83	

TABLE III. Binding energies of $d^3\mathrm{He}\mu$ for $L=0$.

Method	E (eV)	$\Delta E/E$ (%)
EAA	−77.72	+9.87
UAA	−70.45	−0.41
BO [9]	−69.5	−1.75
BO [10]	−69.96	−1.10
Variational [11]	−70.74	

CRG 930102. This work was partly supported by the Deutsche Forschungsgemeinschaft.

APPENDIX

The transformation of the Jacobi coordinates between the different sets is given by

$$\begin{pmatrix} \vec{x}_\beta \\ \vec{y}_\beta \end{pmatrix} = \begin{pmatrix} -c_{\beta\alpha} & d_{\beta\alpha} \\ -d_{\beta\alpha} & -c_{\beta\alpha} \end{pmatrix} \begin{pmatrix} \vec{x}_\alpha \\ \vec{y}_\alpha \end{pmatrix}, \tag{A1}$$

with the constants

$$\begin{aligned} c_{\beta\alpha} &= \sqrt{\frac{m_\alpha m_\beta}{(m_\alpha+m_\gamma)(m_\beta+m_\gamma)}}, \\ d_{\beta\alpha} &= \sqrt{\frac{m_\gamma(m_\alpha+m_\beta+m_\gamma)}{(m_\alpha+m_\gamma)(m_\beta+m_\gamma)}}, \end{aligned} \tag{A2}$$

where (β,α) means (2,1), (3,2), or (1,3). This transformation is orthogonal, i.e., $c_{\beta\alpha}^2+d_{\beta\alpha}^2=1$, and its inverse is given via $c_{\alpha\beta}=c_{\beta\alpha}$ and $d_{\alpha\beta}=-d_{\beta\alpha}$. The hyperradius ρ is invariant with respect to the set of coordinates, while the hyperangle transforms as

$$\begin{aligned} \cos^2\omega_\beta = c_{\beta\alpha}^2\cos^2\omega_\alpha + d_{\beta\alpha}^2\sin^2\omega_\alpha \\ -2c_{\beta\alpha}d_{\beta\alpha}z_\alpha\cos\omega_\alpha\sin\omega_\alpha, \end{aligned} \tag{A3}$$

where $z_\alpha=\hat{x}_\alpha\hat{y}_\alpha$.

Due to the partial wave expansion employed, each element of the matrices $\mathscr{A}$ and $\mathscr{B}$ in Eq. (39) contains an integral of the following structure

$$\begin{aligned} \mathscr{T}^{LM}_{l_\alpha L_\alpha l_\beta L_\beta}(\omega_\alpha) = \int d\hat{x}_\alpha d\hat{y}_\alpha \mathscr{Y}^{LM*}_{l_\alpha L_\alpha}(\hat{x}_\alpha,\hat{y}_\alpha) \\ \times f(\omega_\alpha,z_\alpha)\mathscr{Y}^{LM}_{l_\beta L_\beta}(\hat{x}_\beta,\hat{y}_\beta) \end{aligned} \tag{A4}$$

or

$$\begin{aligned} \mathscr{J}^{LM}_{l_\alpha L_\alpha l'_\alpha L'_\alpha}(\omega_\alpha) = \int d\hat{x}_\alpha d\hat{y}_\alpha \mathscr{Y}^{LM*}_{l_\alpha L_\alpha}(\hat{x}_\alpha,\hat{y}_\alpha) \\ \times f(\omega_\alpha,z_\alpha)\mathscr{Y}^{LM}_{l'_\alpha L'_\alpha}(\hat{x}_\alpha,\hat{y}_\alpha), \end{aligned} \tag{A5}$$

with some function f depending only on ω_α and z_α, a fact holding for all central potentials. Using straightforward algebra, these four-dimensional integrals can be reduced to one-dimensional ones,

$$\begin{aligned} \mathscr{T}^{LM}_{l_\alpha L_\alpha l_\beta L_\beta}(\omega_\alpha) = \sum_{l_x} \mathscr{S}^{l_\alpha L_\alpha L}_{l_\beta L_\beta l_x}(\omega_\alpha) \\ \times \int_{-1}^{1} dz_\alpha P_{l_x}(z_\alpha) \frac{f(\omega_\alpha,z_\alpha)}{\cos^{l_\beta}\omega_\beta \sin^{L_\beta}\omega_\beta}, \end{aligned} \tag{A6}$$

where $P_l(z)$ denotes a Legendre polynomial and

$$\begin{aligned} \mathscr{S}^{l_\alpha L_\alpha L}_{l_\beta L_\beta l_x}(\omega_\alpha) = \frac{(-1)^{L+l_x}}{2}\hat{l}_\alpha\hat{L}_\alpha\hat{l}_\beta^2\hat{L}_\beta^2\hat{l}_x^2 \sum_{l'_\beta L'_\beta} (-1)^{l'_\beta}\sqrt{\begin{pmatrix} 2l_\beta \\ 2l'_\beta \end{pmatrix}\begin{pmatrix} 2L_\beta \\ 2L'_\beta \end{pmatrix}} c_{\beta\alpha}^{l_\beta-l'_\beta+L'_\beta} d_{\beta\alpha}^{l'_\beta+L_\beta-L'_\beta} (\cos\omega_\alpha)^{l_\beta-l'_\beta+L_\beta-L'_\beta} (\sin\omega_\alpha)^{l'_\beta+L'_\beta} \\ \times \sum_{l'_x l'_y} \hat{l}_x'^2\hat{l}_y'^2 \begin{pmatrix} l_\beta-l'_\beta & L_\beta-L'_\beta & l'_x \\ 0 & 0 & 0 \end{pmatrix}\begin{pmatrix} l'_\beta & L'_\beta & l'_y \\ 0 & 0 & 0 \end{pmatrix}\begin{pmatrix} l_\alpha & l'_x & l_x \\ 0 & 0 & 0 \end{pmatrix}\begin{pmatrix} L_\alpha & l'_y & l_x \\ 0 & 0 & 0 \end{pmatrix}\begin{Bmatrix} l'_x & l'_y & L \\ L_\alpha & l_\alpha & l_x \end{Bmatrix} \\ \times \begin{Bmatrix} l'_x & l'_y & L \\ l_\beta-l'_\beta & l'_\beta & l_\beta \\ L_\beta-L'_\beta & L'_\beta & L_\beta \end{Bmatrix}. \end{aligned} \tag{A7}$$

The second integral is simpler since it contains only functions belonging to the same set of coordinates. It reads

$$\mathscr{J}^{LM}_{l_\alpha L_\alpha l'_\alpha L'_\alpha}(\omega_\alpha) = \sum_{l_x} \mathscr{T}^{l_\alpha L_\alpha L}_{l'_\alpha L'_\alpha l_x} \int_{-1}^{1} dz_\alpha P_{l_x}(z_\alpha) f(\omega_\alpha,z_\alpha) \tag{A8}$$

with

$$\mathscr{T}^{l_\alpha L_\alpha L}_{l'_\alpha L'_\alpha l_x} = \frac{(-1)^{L+l_x}}{2}\hat{l}_\alpha\hat{L}_\alpha\hat{l}'_\alpha\hat{L}'_\alpha\hat{l}_x^2 \begin{pmatrix} l_\alpha & l'_\alpha & l_x \\ 0 & 0 & 0 \end{pmatrix}\begin{pmatrix} L_\alpha & L'_\alpha & l_x \\ 0 & 0 & 0 \end{pmatrix}\begin{Bmatrix} l'_\alpha & L'_\alpha & L \\ L_\alpha & l_\alpha & l_x \end{Bmatrix}. \tag{A9}$$

Note that, due to the triangle relations the angular momenta fulfill, all sums appearing in Eqs. (A6)–(A9) are finite. The matrix elements of matrix $\mathscr{A}$ in Eq. (39) are given by

$$\mathscr{A}^{\alpha l_\alpha L_\alpha}_{\beta l_\beta L_\beta i_\beta n}(\rho,\omega_\alpha) = [\tilde{\mathscr{A}}^{\alpha l_\alpha L_\alpha}_{\beta l_\beta L_\beta i_\beta n}(\rho,\omega_\alpha) + \tilde{\mathscr{C}}^{\alpha l_\alpha L_\alpha}_{\beta l_\beta L_\beta i_\beta n}(\rho,\omega_\alpha)]\delta_{\alpha\beta} + \tilde{\mathscr{D}}^{\alpha l_\alpha L_\alpha}_{\beta l_\beta L_\beta i_\beta n}(\rho,\omega_\alpha)\bar{\delta}_{\alpha\beta} \tag{A10}$$

with

$$\tilde{\mathscr{A}}^{\alpha l_\alpha L_\alpha}_{\alpha l'_\alpha L'_\alpha i'_\alpha n}(\rho,\omega_\alpha)=\int d\hat{x}_\alpha d\hat{y}_\alpha \mathscr{Y}^{LM*}_{l_\alpha L_\alpha}(\hat{x}_\alpha,\hat{y}_\alpha)\left[\frac{\Lambda^2}{\rho^2}+V_\alpha\right]e^{-\sqrt{|\epsilon_m|}\rho\cos\omega_\alpha}\cos^{l'_\alpha}\omega_\alpha\sin^{L'_\alpha}\omega_\alpha S_{i'_\alpha}(\omega_\alpha)\mathscr{Y}^{LM}_{l'_\alpha L'_\alpha}(\hat{x}_\alpha,\hat{y}_\alpha)$$

$$=\delta_{l_\alpha l'_\alpha}\delta_{L_\alpha L'_\alpha}\frac{\cos^{l_\alpha}\omega_\alpha\sin^{L_\alpha}\omega_\alpha}{\rho^2}e^{-\sqrt{|\epsilon_m|}\rho\cos\omega_\alpha}\left(\left\{(l_\alpha+L_\alpha+2)^2-\frac{1}{4}-\frac{2\mu_\alpha Z_1\rho}{Z_\alpha\cos\omega_\alpha}-2\rho\sqrt{|\epsilon_m|}\right.\right.$$
$$\times\left[\left(L_\alpha+\frac{3}{2}\right)\cos\omega_\alpha-(l_\alpha+1)\frac{\sin^2\omega_\alpha}{\cos\omega_\alpha}\right]-\rho^2\sin^2\omega_\alpha|\varepsilon_m|\left.\right\}S_{i'_\alpha}(\omega_\alpha)-2\left[(L_\alpha+1)\frac{\cos\omega_\alpha}{\sin\omega_\alpha}-(l_\alpha+1)\frac{\sin\omega_\alpha}{\cos\omega_\alpha}\right.$$
$$\left.\left.+\rho\sin\omega_\alpha\sqrt{|\epsilon_m|}\right]S'_{i'_\alpha}(\omega_\alpha)-S''_{i'_\alpha}(\omega_\alpha)\right)\ , \tag{A11}$$

$$\tilde{\mathscr{C}}^{\alpha l_\alpha L_\alpha}_{\alpha l'_\alpha L'_\alpha i'_\alpha n}(\rho,\omega_\alpha)=\int d\hat{x}_\alpha d\hat{y}_\alpha \mathscr{Y}^{LM*}_{l_\alpha L_\alpha}(\hat{x}_\alpha,\hat{y}_\alpha)\left[\sum_{\beta\neq\alpha}(1-\xi_\beta)V_\beta\right]e^{-\sqrt{|\epsilon_m|}\,\rho\cos\omega_\alpha}\cos^{l'_\alpha}\omega_\alpha\sin^{L'_\alpha}\omega_\alpha S_{i'_\alpha}(\omega_\alpha)\mathscr{Y}^{LM}_{l'_\alpha L'_\alpha}(\hat{x}_\alpha,\hat{y}_\alpha)$$

$$=-\frac{2Z_1}{\rho}\ e^{-\sqrt{|\epsilon_m|}\rho\cos\omega_\alpha}\cos^{l'_\alpha}\omega_\alpha\sin^{L'_\alpha}\omega_\alpha S_{i'_\alpha}(\omega_\alpha)\int d\hat{x}_\alpha d\hat{y}_\alpha\mathscr{Y}^{LM*}_{l_\alpha L_\alpha}(\hat{x}_\alpha,\hat{y}_\alpha)$$
$$\times\left[\frac{\mu_\beta}{Z_\beta\cos\omega_\beta}(1-\xi_\beta)+\frac{\mu_\gamma}{Z_\gamma\cos\omega_\gamma}(1-\xi_\gamma)\right]\mathscr{Y}^{LM}_{l'_\alpha L'_\alpha}(\hat{x}_\alpha,\hat{y}_\alpha)$$

$$=-\frac{2Z_1}{\rho}\ e^{-\sqrt{|\epsilon_m|}\rho\cos\omega_\alpha}\cos^{l'_\alpha}\omega_\alpha\sin^{L'_\alpha}\omega_\alpha S_{i'_\alpha}(\omega_\alpha)$$
$$\times\sum_{l_x}\mathscr{T}^{l_\alpha L_\alpha L}_{l'_\alpha L'_\alpha l_x}\int_{-1}^{1}dz_\alpha P_{l_x}(z_\alpha)\left[\frac{\mu_\beta}{Z_\beta\cos\omega_\beta}(1-\xi_\beta)+\frac{\mu_\gamma}{Z_\gamma\cos\omega_\gamma}(1-\xi_\gamma)\right]\ , \tag{A12}$$

and

$$\tilde{\mathscr{D}}^{\alpha l_\alpha L_\alpha}_{\beta l_\beta L_\beta i_\beta n}(\rho,\omega_\alpha)=\int d\hat{x}_\alpha d\hat{y}_\alpha\mathscr{Y}^{LM*}_{l_\alpha L_\alpha}(\hat{x}_\alpha,\hat{y}_\alpha)\xi_\alpha V_\alpha e^{-\sqrt{|\epsilon_m|}\rho\cos\omega_\beta}\cos^{l_\beta}\omega_\beta\sin^{L_\beta}\omega_\beta S_{i_\beta}(\omega_\beta)\mathscr{Y}^{LM}_{l_\beta L_\beta}(\hat{x}_\beta,\hat{y}_\beta)$$

$$=-\frac{2\mu_\alpha Z_1}{Z_\alpha\rho\cos\omega_\alpha}\xi_\alpha\int d\hat{x}_\alpha d\hat{y}_\alpha\mathscr{Y}^{LM*}_{l_\alpha L_\alpha}(\hat{x}_\alpha,\hat{y}_\alpha)[e^{-\sqrt{|\epsilon_m|}\rho\cos\omega_\beta}\cos^{l_\beta}\omega_\beta\sin^{L_\beta}\omega_\beta S_{i_\beta}(\omega_\beta)]$$
$$\times\mathscr{Y}^{LM}_{l_\beta L_\beta}(\hat{x}_\beta,\hat{y}_\beta)$$

$$=-\frac{2\mu_\alpha Z_1}{Z_\alpha\rho\cos\omega_\alpha}\xi_\alpha\sum_{l_x}\mathscr{S}^{l_\alpha L_\alpha L}_{l_\beta L_\beta l_x}(\omega_\alpha)\int_{-1}^{1}dz_\alpha P_{l_x}(z_\alpha)e^{-\sqrt{|\epsilon_m|}\rho\cos\omega_\beta}S_{i_\beta}(\omega_\beta)\ . \tag{A13}$$

The matrix $\mathscr{B}$ in Eq. (39) is given by

$$\mathscr{B}^{\alpha l_\alpha L_\alpha}_{\beta l_\beta L_\beta i_\beta n}(\rho,\omega_\alpha)=\delta_{\alpha\beta}\delta_{l_\alpha l_\beta}\delta_{L_\alpha L_\beta}e^{-\sqrt{|\epsilon_m|}\rho\cos\omega_\alpha}\cos^{l_\alpha}\omega_\alpha\sin^{L_\alpha}\omega_\alpha S_{i_\alpha}(\omega_\alpha)\ . \tag{A14}$$

[1] S. A. Alexander and H. J. Monkhorst, Phys. Rev. A **38**, 26 (1988).
[2] M. Kamimura, Phys. Rev. A **38**, 621 (1988).
[3] A. M. Frolov and V. D. Efros, J. Phys. B **18**, L265 (1985).
[4] A. K. Bhatia and R. J. Drachman, Phys. Rev. A **30**, 2138 (1984).
[5] V. V. Gusev, V. I. Puzynin, V. V. Kostrykin, A. A. Kvitsinsky, S. P. Merkuriev, and L. I. Ponomarev, Few-Body Syst. **9**, 137 (1990).
[6] M. I. Haftel and V. B. Mandelzweig, Phys. Rev. A **41**, 2339 (1990).
[7] C.-Y. Hu and A. A. Kvitsinsky, Phys. Rev. A **46**, 7301 (1992).
[8] W. H. Breunlich, P. Kammel, J. S. Cohen, and M. Leon, Ann. Rev. Nucl. Part. Sci. **39**, 311 (1989).
[9] Yu. A. Aristov, A. V. Kravtsov, N. P. Popov, G. E. Solyakin, N. F. Truskova, and M. P. Faĭfman, Yad. Fiz. **33**, 1066 (1981) [Sov. J. Nucl. Phys. **33**, 564 (1981)].
[10] S. S. Gershtein and V. V. Gusev, IHEP Report No. 92-129, (1992) (unpublished).
[11] S. Hara and T. Ishihara, Phys. Rev. A **39**, 5633 (1989).
[12] J. Macek, J. Phys. B **1**, 831 (1968).
[13] D. M. Hood and A. Kuppermann, *Theory of Chemical Reaction Dynamics*, (Reidel, Boston, 1986), p. 193.
[14] V. G. Galerkin, Vestnik Inzhenerov **1**, 897 (1915); H.-J. Reinhardt, *Analysis of Approximation Methods for Differential and Integral Equations*, Springer Series on Applied Mathematical

Sciences Vol. 57 (Springer, Berlin, 1985).
[15] T. K. Das, H. T. Coelho, and M. Fabre de la Ripelle, Phys. Rev. C **26**, 2281 (1982).
[16] A. A. Kvitsinsky and V. V. Kostrykin, J. Math. Phys. **32**, 2802 (1991).
[17] H. T. Coelho and J. E. Hornos, Phys. Rev. A **43**, 6379 (1991).
[18] M. Fabre de la Ripelle and J. Navarro, Ann. Phys. (N.Y.) **123**, 185 (1979).
[19] C. D. Lin, Phys. Rev. A **23**, 1585 (1981).
[20] V. B. Belyaev, M. Decker, H. Haberzettl, L. J. Khaskilevitch, and W. Sandhas, Few-Body Syst. Suppl. **6**, 332 (1992).
[21] H. R. Sadeghpour, Phys. Rev. A **43**, 5821 (1991).
[22] L. D. Faddeev, Zh. Éksp. Teor. Fiz. **39**, 1459 (1961) [Sov. Phys. JETP **12**, 1014 (1961)].
[23] H. P. Noyes, and H. Fiedeldey, *Three-Particle Scattering in Quantum Mechanics* (Benjamin, Reading, 1968).
[24] S. P. Merkuriev, Ann. Phys. (N.Y.) **130**, 395 (1980).
[25] A. A. Kvitsinsky, J. Carbonell, and C. Gignoux, Phys. Rev. A **46**, 1310 (1992).
[26] C. de Boor, *A Practical Guide to Splines* (Springer, Berlin, 1978).
[27] M. Decker, Ph.D. thesis, Bonn University, 1994.
[28] G. L. Payne, *Configuration-space Faddeev Calculations: Numerical Methods*, Lecture Notes in Physics Vol. 273 (Springer, Berlin, 1987), p. 64.
[29] Y. Kino and M. Kamimura, Hyperfine Interact. **82**, 195 (1993).
[30] V. B. Belyaev, O. I. Kartavtsev, V. I. Kochkin, and E. A. Kolganova, Phys. Rev. A **52**, 1765 (1995).
[31] T. Kato, Commun. Pure Appl. Math. **10**, 151 (1957).
[32] C. R. Myers, C. J. Umrigar, J. P. Sethna, and J. D. Morgan III, Phys. Rev. A **44**, 5537 (1991).